Environmental Pollution 286 (2021) 117195

Contents lists available at ScienceDirect

Environmental Pollution

journal homepage: www.elsevier.com/locate/envpol

Primary and secondary aerosols in small passenger vehicle emissions: Evaluation of engine technology, driving conditions, and regulatory standards☆

Gyutae Park [a], Kyunghoon Kim [a], Taehyun Park [a], Seokwon Kang [a], Jihee Ban [a], Siyoung Choi [a], Dong-Gil Yu [a], Sanguk Lee [b], Yunsung Lim [b], Sunmoon Kim [b], Sunhee Mun [b], Jung-Hun Woo [c], Chan-Soo Jeon [d], Taehyoung Lee [a,*]

[a] Department of Environmental Science, Hankuk University of Foreign Studies, Yongin, 17035, South Korea
[b] Transportation Pollution Research Center, National Institute of Environmental Research, Incheon, 22689, South Korea
[c] Department of Civil and Environmental Engineering, Konkuk University, Seoul, 05029, South Korea
[d] Korea Institute of Civil Engineering and Building Technology, Goyang, 10223, South Korea

ARTICLE INFO

Keywords:
Potential aerosol mass (PAM)
Secondary organic aerosol (SOA)
Liquefied petroleum gas (LPG)
Expected SOA yield
Korean small passenger vehicles

ABSTRACT

The characteristics of primary gas/aerosol and secondary aerosol emissions were identified for small passenger vehicles using typical fuel types in South Korea (gasoline, liquefied petroleum gas (LPG), and diesel). The generation of secondary organic aerosol (SOA) was explored using the potential aerosol mass (PAM) oxidation flow reactor. The primary emissions did not vary significantly between fuel types, combustion technologies, or aftertreatment systems, while the amount of NH_3 was higher in gasoline and LPG vehicle emissions than that in diesel vehicle emissions. The SOA emission factor was 11.7–66 mg kg-fuel^{-1} for gasoline vehicles, 2.4–50 mg kg-fuel^{-1} for non-diesel particulate filter (non-DPF) diesel vehicles (EURO 2–3), 0.4–40 mg kg-fuel^{-1} for DPF diesel vehicles (EURO 4–6), and 3–11 mg kg-fuel^{-1} for LPG vehicles (lowest). The carbonaceous aerosols (equivalent black carbon (eBC) + primary organic aerosol + SOA) of diesel vehicles in EURO 4–6 were reduced by up to 95% compared to those in EURO 2–3. The expected SOA yield increased through the hot-condition combustion section of a vehicle, over the SOA range of 0.2–155 μg m^{-3}. These results provide the necessary data to analyze all types of SOA generated by the gas-phase oxidation in vehicle emissions in metropolitan areas.

1. Introduction

Vehicles directly cause air pollution by emitting nitrogen oxides (NO_x), carbon monoxide (CO), volatile organic compounds (VOCs), and particulate matter (PM). These emissions also contribute to secondary air pollution by chemically reacting with air pollutants from various sources (Deng et al., 2020; George et al., 2015; Saha et al., 2018a, 2018b). Furthermore, as vehicles are the source of air pollution most closely related to people's daily lives in urban aera, the level of corresponding risk perceived by the public is higher than that from other sources (e.g., combustion in energy and transformation industry, combustion in manufacturing industry, and non industrial combustion) (Heal et al., 2012). For this reason, vehicle emission sources are used as a major instrument in every country's air pollution policy-making. For example, in South Korea, policy is focused on diesel vehicles; if a high concentration of fine dust has been predicted the previous day (Supporting Information, SI, Section S1), diesel vehicles that are not equipped with a diesel particulate filter (DPF) are restricted from 6 a.m. to 9 p.m. in metropolitan areas as the action of Ministry of Environment (MOE) (MOE, 2019). Furthermore, in order to increase the demand for clean fuels, the government has revised the law to allow the general public to purchase liquefied petroleum gas (LPG) vehicles, which were previously only available for commercial use, such as taxis. The aim of this revision was to encourage the purchase of LPG vehicles instead of diesel vehicles, as the latter produce fine dust.

In South Korea LPG is classified as a clean fuel, which has main ingredients being propane (C_3H_8) and butane (C_4H_{10}), and also contains some low C4–C5 carbons. These compounds are highly volatile, which

☆ This paper has been recommended for acceptance by Pavlos Kassomenos.

* Corresponding author.
E-mail address: thlee@hufs.ac.kr (T. Lee).

https://doi.org/10.1016/j.envpol.2021.117195
Received 2 February 2021; Received in revised form 1 April 2021; Accepted 19 April 2021
Available online 3 May 2021

increases the probability of a homogenous mix during the combustion process and enables complete combustion. In this regard, Myung et al. (2014) compared domestic LPG vehicles and gasoline vehicles with gasoline direct injection (GDI) engines, and reported that total hydrocarbons (THC), CO, and NO_x emissions were 13 times, 2.6 times, and 13.3 times lower for LPG vehicles, respectively; further, the number of particles decreased by approximately 99% (from 4.57×10^{11}–1.01×10^{12} N km^{-1} to 2.53×10^{9}–1.07×10^{10}) in case of LPG vehicles. Park et al. (2019) reported that in hot conditions the NO_x emission of LPG vehicles was 0.01 ± 0.006 g km^{-1}, approximately 69 times lower than that of diesel vehicles in EURO 5 and 6 (0.65 ± 0.47 g km^{-1}) and at a similar level to gasoline vehicles. The gravimetric PM results obtained from filter measurements for LPG vehicles were 2.8 times lower (2.101 mg km^{-1} and 0.757 mg km^{-1}) than those obtained from gasoline vehicles with a GDI engine running in the Constant Volume Sampler-75 (CVS-75, same as the Federal Test Procedure (FTP-75) of U.S. Environmental Protection Agency (EPA)) and 1.2 times lower (0.656 mg km^{-1} and 0.539 mg km^{-1}) in the highway mode (Myung et al., 2012). Considering these results, LPG vehicles are more environmentally friendly than diesel and gasoline vehicles and are in line with domestic policy directions. However, there are insufficient data regarding the formation of secondary aerosols in the atmosphere due to LPG vehicle emissions, relative to gasoline and diesel vehicles. Therefore, more relevant research into LPG vehicles is needed to allow for a comprehensive evaluation.

Various studies have investigated the formation of secondary aerosols from gasoline and diesel vehicles, ranging from smog chamber experiments to recently-developed oxidation flow reactor (OFR) studies. The research results on the chassis-dynamometer related to this study have been briefly reviewed, and the New European Driving Cycle (NEDC) results in a smog chamber study conducted by Platt et al. (2017) showed that the carbonaceous (BC, primary organic aerosol (POA), and secondary organic aerosol (SOA)) emissions of gasoline vehicles with direct injection (DI) and port fuel injection (PFI) combustion methods of EURO 5 were ten times higher than those of diesel vehicles equipped with DPF at 22 °C, and 62 times higher at −7 °C. In addition, Zhao et al. (2018) used an OFR to show that, as the non-methane organic gas (NMOG) regulatory standard for gasoline vehicles was strengthened from pre-low emission vehicle (pre-LEV) to super ultra-low emission vehicle (SULEV), the production of SOA decreased, but there was no significant difference in the production volume and SOA yield between GDI and PFI combustion methods. In addition, Karjalainen et al. (2019) conducted a study that simulated the combination of aftertreatment systems (which became common when emission regulations were introduced for diesel engines). They reported that, when progressing from no aftertreatment system and diesel oxidation catalyst (DOC) systems to combinations of DOC + selective catalytic reduction (SCR) and DOC + DPF + SCR systems, the total PM including SOA (refractory BC (rBC), organic matter, sulfate, nitrate, and ammonium) was reduced by up to 100% (from 106.2 mg kWh^{-1} to almost 0 mg kWh^{-1}). The research results of gasoline and diesel vehicles based on various other parameters, such as the type of vehicle, model year, and driving mode, form an important basis for assessing the air pollution levels of countries or metropolitan areas (Giani et al., 2019; Jathar et al., 2014; Karjalainen et al., 2019; Platt et al., 2017; Zhao et al., 2017).

However, the main types of fuel for vehicles operating in Korea are gasoline (46.3%), diesel (42.1%), and LPG (8.5%; Table S1), which lack research data that could be used as the basis for identifying the primary and secondary air pollution effects caused by the combinations of different emissions. Therefore, in this study, small passenger vehicles using gasoline, LPG, and diesel were divided by engine technology and regulatory standards, and their emission production and secondary formation were investigated depending on the regulatory standard mode, using a chassis dynamometer. The PAM oxidation flow reactor (Aerodyne, Inc) was used to simulate the secondary formation, and the level of SOA formation was analyzed as a function of photochemical reaction time in a simulated atmosphere, in conjunction with the precursor gas results. In addition, comparisons were made regarding the formation of SOA from combustion emissions from each fuel type, and a comprehensive evaluation was conducted on the exhaust emissions of domestic passenger vehicles regarding the formation of SOA.

2. Experimental section

2.1. Test configuration

Domestic gasoline and LPG vehicles were subjected to U.S. emissions regulations, while diesel vehicles were subjected to EU regulations, requiring the classifications of vehicles to correspond to each regulation. To ensure the representativeness of the results, 16 small passenger vehicles that held high market shares in Korea were ultimately selected (Table S2). Among the five gasoline vehicles with different regulations and combustion technologies, two were PFI vehicles satisfying LEV out of LEV1, two had GDI combustion methods, and one had a PFI combustion method that satisfied the ultra-low emission vehicle (ULEV) standard of LEV2. The two GDIs were divided into GDI-BF-ULEV before being subjected to the PM regulations for GDIs in South Korea (0.004 g km^{-1} after 2014), and GDI-AF-ULEV after being subjected to the regulation (Park et al., 2019, 2020). The two LPG vehicles fell under the ULEVs of LEV2; they employed LPG injection (LPI) engine technology to inject LPG directly into the combustion chamber. Nine diesel vehicles were classified into EURO 2–6. In EURO 6, there was one vehicle with an aftertreatment system combination of DOC + Lean NO_x Trap (LNT) + DPF and two vehicles with a combination of DOC + DPF + SCR. Information regarding their fuel properties is provided in section S2. When preparing the test vehicles, CVS-75 and the EU NEDC were applied in the driving mode to assess the emission regulatory standards (section S3 and Fig S1). The emission regulation standards for the vehicles used in this study are presented in Table S4, alongside information for CVS-75 and NEDC.

2.2. Measurement system

The study was conducted at the Transportation Pollution Research Center of the National Institute of Environmental Research (NIER) in Incheon, South Korea. Test vehicles were driven twice per CVS-75 and NEDC mode using a chassis dynamometer and a CVS system. The first tests of each modes were conducted without the PAM and the second tests were used the PAM. In the whole experiments, the gases and equivalent black carbon (eBC) were measured prior to the PAM, so they were defined as the primary emission. Here, the aerosol in the first test was included in the primary emission and the aerosol passing through the PAM was considered to be the secondary emissions. In this paper, we report comprehensive eBC trend for vehicle emissions by integrating recently published data of eBC emission (Park et al., 2020), and expanding the vehicles in this study (Table S2).

Further dilution was made for the old diesel vehicles with high-concentration emissions in EURO 2 and 3. High-purity dried zero air, Supelpure® hydrocarbon trap (Sulpelco), and a humidifier (Perma Pure, LLC) were mixed with exhaust gas to dilute said emissions, for 9 to 17-time dilutions. The general instrument information of the gases and particles in this study are detailed in section S4. The NH_3 measurements were collected directly from the tailpipe of each vehicle, based on the measurement code described by Link et al. (2017). The aerosol components of the primary and secondary emissions were measured using a High Resolution Time-of-Flight Aerosol Mass Spectrometer (HR-To-F-AMS, Aerodyne Research, Inc.), a detailed description of which is provided in many studies (DeCarlo et al., 2006; Deng et al., 2020; Hu et al., 2016; Jathar et al., 2014; Karjalainen et al., 2019; Link et al., 2017; Liu et al., 2019; Pieber et al., 2018; Platt et al., 2017; Zhao et al., 2017, 2018). Organics, nitrate, sulfate, ammonium, and chloride in the aerosol were measured at 1-min intervals in the V-mode, and the data

were treated using the software packages SQUIRREL (version 1.62F) and PIKA (version 1.22F) in the HR-ToF-AMS toolkit of Igor Pro (version 7.08). Additional details of the HR-ToF-AMS are provided in section S4.

In this study, the PAM was deployed for forming the secondary aerosol as the one kind of the oxidation flow reactors. The PAM was designed according to Kang et al. (2007, 2011), and has since been upgraded and commercialized by Aerodyne Research, Inc. It is currently used by more than 40 research groups across various fields, such as aircraft, field, source, and laboratory (Kang et al., 2011; Nault et al., 2018; Saha et al., 2018a,b; Shah et al., 2019; Tkacik et al., 2014; Ylisirniö et al., 2020). While the operation of PAM is known to have various methods depending on the major oxidants, in this study, the OFR254 method was used to produce hydroxyl radicals (OH) (Li et al., 2015). The OH exposure simulated inside PAM ranged from 5.5×10^9 molecules cm^{-3} s to 9.9×10^{11} molecules cm^{-3} s, using a photochemical model (Matlab base) that was improved by Lambe et al. (2011) (section S5 and Fig. S2). The daily OH exposure in the atmosphere used for conversion was 1.5×10^6 molecules cm^{-3}, as suggested by Mao et al. (2009). This corresponded to an average of approximately 7.7 of photochemical aging days.

2.3. Particle emission/production factors

Equation (1), which is based on carbon balance, was used with primary and secondary aerosols and eBC emission/production factors (EF) (mg kg-fuel^{-1}). Primary ΔPA is the background-corrected EF and secondary ΔSA excludes ΔPA and PAM background concentrations ($\mu g\ m^{-3}$). ΔCO_2 and ΔCO were calculated in terms of molecular weights (μg of C m^{-3}) by correcting the background concentrations in the CVS tunnel and MW_C is the molecular weight of carbon. Domestic study results on the carbon content in fuels were used for C_f, including 0.833 for gasoline, 0.824 for LPG, and 0.857 for diesel (Korea Energy Agency, 2014).

$$EF = 10^6 \times \left(\frac{\Delta PA \text{ or } \Delta SA}{\Delta CO_2 + \Delta CO}\right) \times \frac{C_f}{MW_c} \quad (1)$$

2.4. Expected SOA yield

The expected SOA yield is defined as the ratio between the actual measured SOA ($\Delta SOA_{measured}$, $\mu g\ m^{-3}$) and the theoretical SOA ($\Delta SOA_{precursor\text{-}reacted}$, $\mu g\ m^{-3}$) formed during the reaction between the precursor of each SOA and OH radicals (Odum et al., 1996). Here, reacted organic gas (ROG_i) refers to the single compound, i ($\mu g\ m^{-3}$), of the SOA precursor; k_{OH} is the OH reaction rate constant (based on 25 °C, molecules cm^{-3}) of i; and [OH] × Δt is the OH exposure over the residence time inside PAM during the test (Jathar et al., 2017; Zhao et al., 2017, 2018).

$$\Delta\ SOA_{precursor-reacted} = \sum_i ROG_i \times \left(1 - e^{-k_{OH} \times [OH] \times \Delta t}\right) \quad (2)$$

In this study, ROG_i was not measured; instead, the ideal effective SOA yield was calculated by distinguishing the fractions and compositions of the VOCs and intermediate VOCs (IVOCs) among the two modes of non-methane hydrocarbon (NMHC). i) The normalized profiles of gasoline and diesel vehicles, which were expanded to include 200 types of VOC compounds by Lu et al. (2018), were used. ii) In addition to VOCs for gasoline and diesel vehicles, the IVOC compositions and fractions from Zhao et al. (2016, 2015) were used, as recent research has shown that IVOCs are important for explaining SOA precursors in automobile exhaust gases (Robinson et al., 2007). Here, the non-DPF result was used collectively for the fraction of IVOCs for diesel vehicles. This was done because the IVOCs-to-NMHC ratio in DPF was 1 or more on average, and this study was structured around the fraction of IVOCs in NMHC. However, the expected SOA yield in this study obtained using the non-DPF IVOCs fraction was underestimated by 1–3%, compared to when the IVOCs fraction of DPF-equipped diesel vehicles were used, as demonstrated by Zhao et al. (2015). iii) As there were only 12 VOC classifications in the profile 8857–8860 of the EPA's SPECIATE database (version 4.3), the 2015 project results of the NIER-Transportation Pollution Research Center (section S6) were used (Lee et al., 2015) to obtain a broader range of classifications (driving cycle in Fig. S3). Finally, based on the volatility basis set (VBS) results of Lu et al. (2018), IVOCs–to-NMOG ratios of 0.046 and 0.0181 were used in Phases 1 and 2, respectively, for the CVS-75 and NEDC modes of gasoline vehicles. Furthermore, and IVOCs-to-NMOG ratio of 0.542 was applied to EURO 2–3 vehicles without DPF, and a ratio of 0.455 was applied to EURO 4–6 vehicles equipped with DPF (Lu et al., 2018). The VOCs of the LPG vehicles were divided into cold and hot conditions, similar to gasoline vehicles. Only the VOC components were included, as not all cases showed IVOCs (Lee et al., 2015). In addition, due to the combustion characteristics of LPG vehicles, their percentages of methane emissions were high (hot 58%, cold 19%). This was accounted for in the expected SOA yield calculations.

3. Results and discussion

3.1. General gas/particle emissions

Fig. 2 shows the gaseous emission results of gasoline, LPG, and diesel vehicles by regulation mode for NMOG (or NMNHC, as propane), NO_x (as NO_2), CO, CO_2, SO, and direct-NH_3 were measured directly in the tailpipe. To evaluate whether the emission regulation standards were satisfied by each fuel type, the NMOG (or NMHC), CO, and NO_x results were examined (gasoline, LPG, and EURO 3 for CVS-75, EURO 4–6 for NEDC). The PFI-LEV #2 vehicle was found to exceed the CO and NMHC standards (CO = 2610 mg km^{-1}, NMHC = 56 mg km^{-1}; based on the standard of 5 years/80,000 km in SI Table S4) by 110 mg km^{-1} (EF = 2700 mg km^{-1}) and 3 mg km^{-1} (EF = 59 mg km^{-1}), respectively. The NO_x and NMOG emissions of LPI-ULEV #1 exceeded these standards by 6 mg km^{-1} (EF = 39 mg km^{-1}) and 3 mg km^{-1} (EF = 37 mg km^{-1}), respectively. For diesel vehicles, the NO_x emissions of EURO 2 exceeded the given standard by 251 mg km^{-1} (EF = 1271 mg km^{-1}) and the NMHC + NO_x and NO_x emissions of EURO 4 exceeded the given standard by 44 mg km^{-1} (EF = 344 mg km^{-1}) and 89 mg km^{-1} (EF = 339 mg km^{-1}), respectively. Furthermore, the NMHC + NO_x and NO_x emissions of EURO 5 #2 exceeded the given standards by 11 mg km^{-1} (EF = 241 mg km^{-1}) and 25 mg km^{-1} (EF = 205 mg km^{-1}), respectively, and the NO_x emissions of EURO 6-SCR #2 were more than 18 mg km^{-1} (EF = 98 mg km^{-1}) higher than the regulation standard. While the other test vehicles were found to satisfy the regulatory standards, those that exceeded the standards by 4–30% were believed to do so because of the aging and maintenance of their engines, aftertreatment systems, and other accessory devices. It is important to be aware of these individual effects when interpreting these results.

When the general characteristics of the two driving outcomes were examined based on the different regulatory standards, the gasoline and LPG vehicles emitted noticeable amounts of NMOG (or NMHC, gasoline = 13–189 mg km^{-1}, LPG = 17–36 mg km^{-1}), CO (gasoline = 219–5602 mg km^{-1}, LPG = 229–651 mg km^{-1}), and direct-NH_3 (gasoline = ~19.8 ppm, LPG = ~29.5 ppm), while the diesel vehicles emitted relatively higher levels of NO_x (38–1282 mg km^{-1}) and SO_2 (0.4–6.7 mg km^{-1}). The relationships between the NMOG (or NMHC), CO, and NO_x emissions of the gasoline and diesel vehicles were identical to the emission fraction trends of the gasoline and diesel vehicles of EURO 5 and 6 as studied by Platt et al. (2017). Furthermore, the SO_2 and direct-NH_3 emissions were similar to the emissions by fuel type determined under hot conditions by Park et al. (2019). As CO_2 emissions vary in quantity depending on the engine displacement (cc), only the vehicles with displacements of 1900–2000 cc were compared. The emissions of the LPG vehicles at 187–202 mg km^{-1} were slightly lower than those of the gasoline vehicles at 189–258 mg km^{-1} and the diesel vehicles at

187–242 mg km^{-1}. This was likely because the gasoline and diesel vehicles had lower carbon contents, lower heating values, and higher octane numbers than those of LPG vehicles (Myung et al., 2014; Yeom et al., 2007). Regarding greenhouse gases, LPG vehicles may provide a solution to reducing the overall CO_2 emissions of mobile pollutants, while their lower NMOG (or NMHC), SO_2, and NO_x emissions compared to the other fuel types could reduce the effects of the primary air pollution. However, as shown in Fig. 1b, LPG vehicles ultimately contribute more to the emission of pollutants during the cold-start than during the hot-start. This is due to the stabilization of the engine and drive-related systems, and due to the aftertreatment system reaching its optimal activation temperature (Fig. S4). This indicates that the effects of cold-starts should be considered when evaluating the emissions and air pollution of LPG vehicles in the future. In addition, the direct-NH_3 emissions of LPG vehicles, as shown in Figs. 1b and 2, averaged 10–29.5 ppm. This was similar to the average range of gasoline vehicles (1.4–19.8 ppm), which implies that secondary pollution may occur with nitrogen oxides reacting in the atmosphere to produce ammonium nitrate (more details are provided in the secondary aerosol emission section).

Fig. 3 shows the EFs for primary eBC and POA (with background concentrations corrected) and the EFs for SOA and nitrate following PAM. Based on the primary eBC results, the EFs of each type of driving mode and fuel showed similar tendencies. The gasoline regulatory standards indicated different eBC EF and POA EF trends, depending on the combustion technology (PFI or GDI). During the LEV1 stage, the POA EFs of PFI-LEV #1 and #2 ranged from 3.4–11.1 mg kg-fuel^{-1}, which were 2.8–5 times higher than for eBC EF (1.2–25 mg kg-fuel^{-1}). In contrast, the eBC EFs for ULEV vehicles in LEV2 ranged from 0.9–12.5 mg kg-fuel^{-1}, which were 7.6–42.8 times higher than the POA EFs (0.1–1.6 mg kg-fuel^{-1}). This is similar to the reductions in organic carbon (OC)/elemental carbon (EC) (filter measurements) from LEV1 to LEV2 reported by May et al. (2014). It appears to be the result of the improved performance of the overall combustion and aftertreatment systems, due to the tightened regulatory standards.

The GDI vehicles produced eBC EFs of 4.2–12.5 mg kg-fuel^{-1} and POA EFs of 0.1–1.6 mg kg-fuel^{-1}, which were 13.3–14 times higher than those of the PFI vehicles; these findings were similar to those of previous studies (Du et al., 2018; Saliba et al., 2017). The GDI vehicles each had a displacement of 1600 cc; their POA EFs were 9.6 times (1.2–0.12 mg kg-fuel^{-1}, CVS-75) and 10.9 times (1.6–0.15 mg kg-fuel^{-1}, NEDC) lower before and after the PM regulation (4 mg km^{-1}). Furthermore, their eBC EFs decreased by 2.5 times (10.3–4.2 mg kg-fuel^{-1}, CVS-75) and two times (12.5–6.3 mg kg-fuel^{-1}, NEDC) before and after the PM regulation. These reductions could be explained by the findings of Choi et al. (2019), who reported that PM (gravimetric measurement) decreased with increasing injector pressure in the cylinders of GDI vehicles. Furthermore, while OC/EC (filter measurement) was found to be higher, the POA EF-to-eBC EF ratio decreased from 0.13 to 0.02 in this study; further research is needed to fully understand the cause. However, eBC EF + POA EF emitted from the GDI vehicles in this study was 9.12 mg kg-fuel^{-1}, which was approximately 17.4 times higher than that of EURO 4–6 diesel vehicles equipped with DPF (0.53 mg kg-fuel^{-1}). This suggests the significance of the primary particle emissions of GDI regarding air pollution.

In this study, regardless of the vehicle age (MY, 2008, 2014), the POA EFs of the LPG vehicles (0.1–0.4 mg kg-fuel^{-1}) were similar to those of PFI-ULEV. Furthermore, the eBC EFs (0.2–0.3 mg kg-fuel^{-1}) were lower than those of PFI-ULEV. This was because the combustion of LPG is advantageous for the formation of a vapor mixture because of its high steam pressure and vaporization characteristics. Furthermore, its composition is simpler than that of gasoline, which decreases the formation of complex carbon chains during the combustion process (Myung et al., 2012, 2014). The fresh soot emissions of diesel vehicles (in terms of eBC EFs) decreased noticeably by 99.9% following the installation of DPF, from 531 mg kg-fuel^{-1} for non-DPF (EURO 3#1,2) to 0.5 mg kg-fuel^{-1} for DPF (EURO 4–6). Furthermore, the POA EF was 531 mg kg-fuel^{-1} for non-DPF vehicles (EURO 2–3) and 0.15 mg kg-fuel^{-1} (maximum) for DPF vehicles (EURO 4–6), based on the corrected background concentrations.

3.2. Secondary aerosol emissions

Fig. 3 shows the results of the SOA and nitrate EFs calculated using PAM (Table S7). In the two modes, the SOA EFs for gasoline vehicles were highest, at 11.7–66 mg kg-fuel^{-1}, while non-DPF diesel vehicles (EURO 2–3) and DPF diesel vehicles (EURO 4–6) exhibited similar values (2.4–50 and 0.4–40 mg kg-fuel^{-1}, respectively). The SOA EFs of LPG vehicles were estimated to be the lowest (3–11 mg kg-fuel^{-1}). The difference between SOA EFs between gasoline and diesel vehicles in this

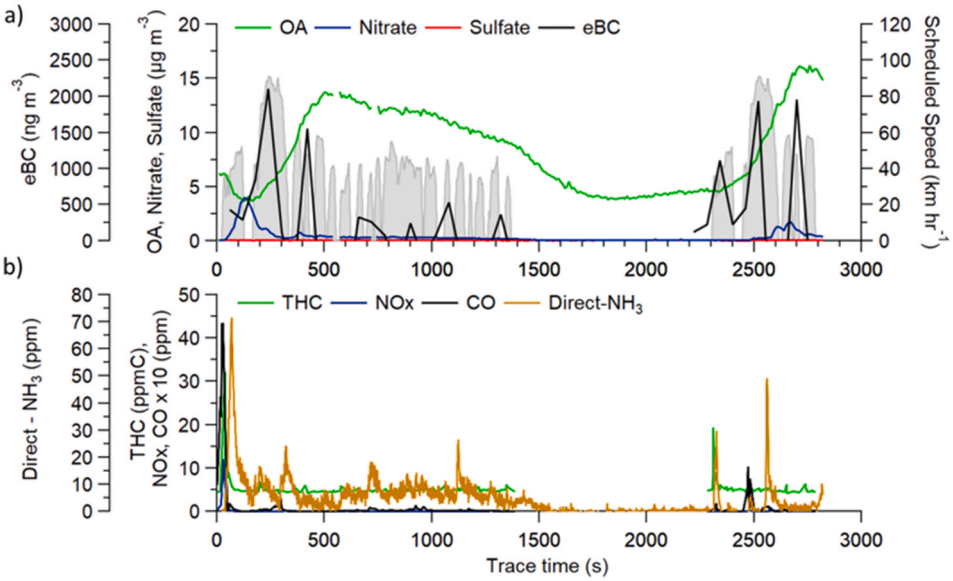

Fig. 1. Raw primary gases and eBC from CVS tunnel, and secondary aerosols with PAM of LPI-ULEV #1. a) Trends of oxidized raw organics, nitrate, and sulfate with PAM from CVS tunnel, and primary eBC from CVS tunnel at driving speed. b) Raw emissions of the primary gases from CVS tunnel; NH_3 was measured directly from the tailpipe.

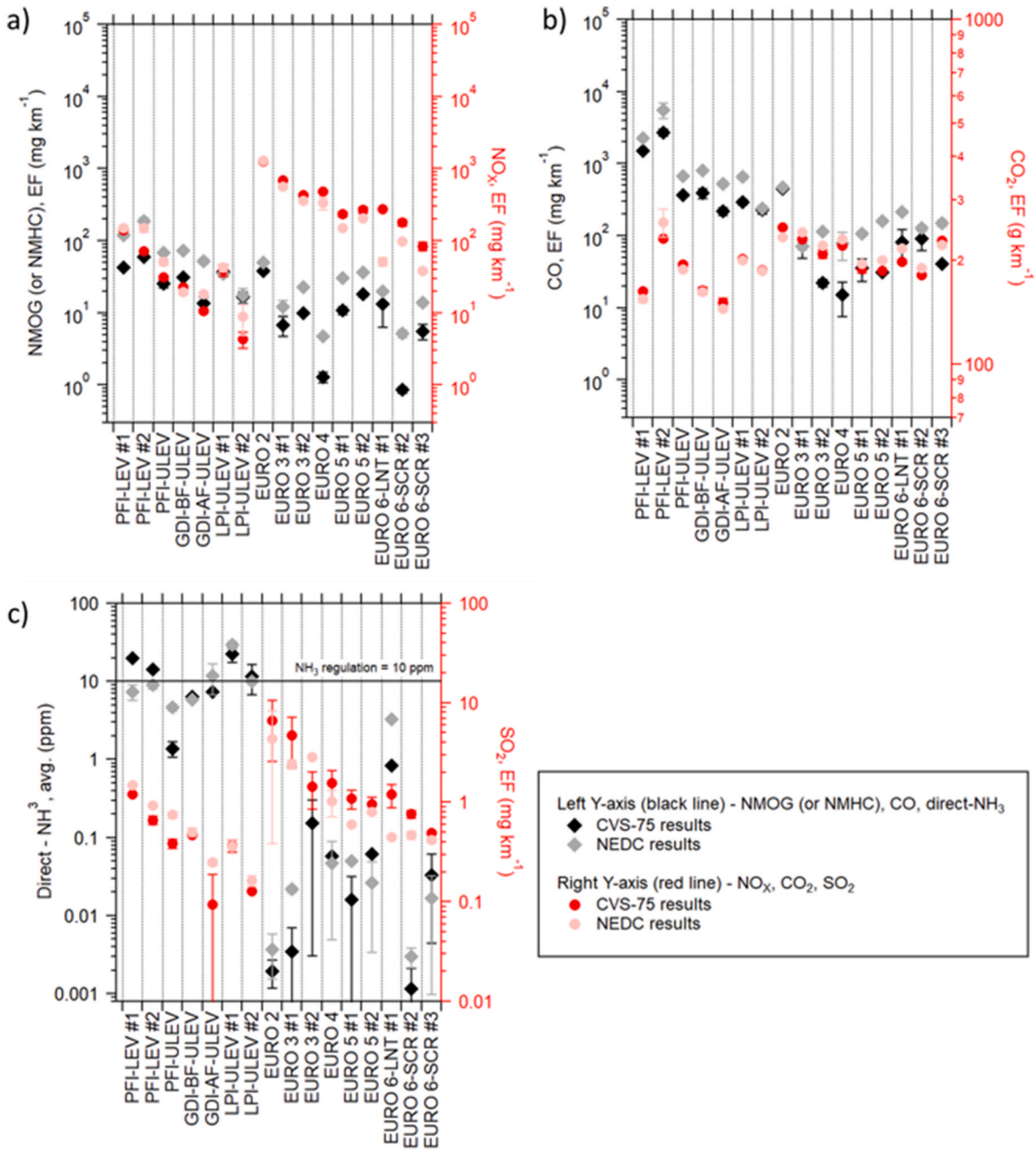

Fig. 2. Final EFs of primary gases by CVS-75 and NEDC, according to the test method procedure in law. a) Left axis shows NMOG or NMHC, calculated by THC plus carbonyls and alcohols minus methane for NMOG, and by THC minus CH_4 for NMHC. NO_x EFs were calculated as NO_2. b) Results of CO and CO_2 were measured using a non-dispersive infrared analyzer. c) NH_3 was directly sampled from the tailpipe. Regulated concentration of NH_3 is below 10 ppm (average value of whole driving) for heavy passenger vehicles and heavy trucks with gross vehicle weight (GVW) over 3500 kg in Korea. Since 2013, this has also applied to gasoline and LPG vehicles manufactured; since 2014 it has applied to diesel vehicles. SO_2 EFs were calculated using the same method as for regulated emissions gases. The detailed emission standard was in Table S4.

study was in agreement with previous studies conducted using smog chambers and PAM (Gordon et al., 2013, 2014a, 2014b; Jathar et al., 2014; May et al., 2014; Platt et al., 2017). However, the NEDC results showed that the SOA EFs of gasoline vehicles were 11.7–38 mg kg-fuel^{-1}, a range similar to that of DPF diesel vehicles (EURO 4–6; 12.8–39.7 mg kg-fuel^{-1}). Platt et al. (2017) indicated that for NEDC results, the EFs (BC + POA + SOA) of gasoline vehicles (PFI, GDI) of EURO 5 were on average ten times higher than those of diesel vehicles (DOC + DPF) at an experimental temperature of 22 °C. However, in this study, the EFs (eBC + POA + SOA) of ULEV gasoline vehicles in LEV2 ranged from 26.1 to 43.3 mg kg-fuel^{-1}, which was only 1.2 times higher than those of EURO 5 vehicles with a combination of DOC and DPF (21.2–30.9 mg kg-fuel^{-1}). While further research may be required, the variables related to the other exhaust gases, such as composition, OH radical concentration, dilution level, maintenance conditions, and combustion systems, may be responsible for this disparity, as in this study the NMHC-to-NO_x ratio ($ppmC_{PAM\ input}/ppm_{PAM\ input}$) ranged from 2 to 24 for the gasoline vehicles and from 0.3 to 1.6 for the diesel vehicles. This was lower than the VOC-to-NO_x ratio at 22 °C for gasoline vehicles (3.1–6.1), and was similar to the range for diesel vehicles reported by Platt et al. (2017) (0.3–11).

Shifting from LEV1 to LEV2, gasoline vehicle emissions showed

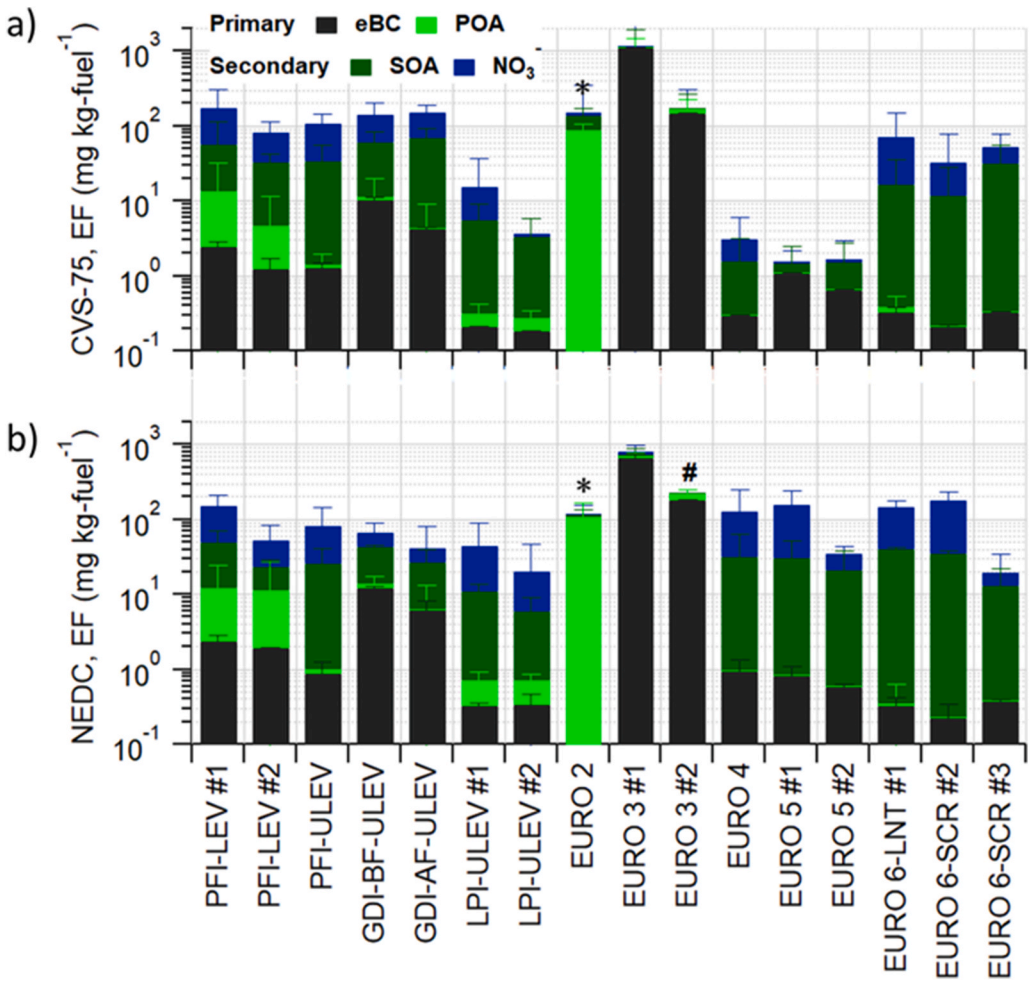

Fig. 3. Average EFs of primary aerosols (eBC and POA), and secondary aerosols (organics and nitrate); corrected background data from CVS-75 and NEDC are shown. a) For CVS-75, not considering the weight factor. b) For NEDC. *No data for eBC, # only primary aerosols (eBC and POA) were available due to failure of PAM measurement.

increase in NMOG levels (NMHC for LEV of LEV1 phase; NMOG for ULEV of LEV2 phase from gasoline and LPG vehicles in the Korean regulations) by 39% (0.056–0.034 g km^{-1} by the standard, based on 80,000 km/five years). However, the overall SOA EF increased from 30.6 mg kg-fuel^{-1} to 37.1 mg kg-fuel^{-1}. This may the result of the decreased POA EF concentrations (3.4–11.1 mg kg-fuel^{-1} for LEV, 0.1–1.6 mg kg-fuel^{-1} for ULEV) affecting the SOA EF, as shown in Eq. (1) (e.g., SOA EF/POA EF increased from 1.2 to 8.2 to 41.2–531). Furthermore, the fraction of the SOA precursors in NMOG (or NMHC) either remained the same or increased because of higher carbon contents and enhanced aftertreatment systems, even though NMOG was reduced to meet the tightened regulation (Gordon et al., 2014a; Jathar et al., 2014; Zhao et al., 2017).

The SOA EF of LPG vehicles was (on average) 6.1 mg kg-fuel^{-1}, which was six times lower than those of gasoline and EURO 4–6 diesel vehicles in ULEV. Considering the similar OH exposures of the subject vehicles during the experiment (7×10^{11} for LPG vehicles, 8.8×10^{11} for ULEVEs of gasoline vehicles, and 9.9×10^{11} molecules cm^{-3} s for EURO 4–6 diesel vehicles), the SOA EFs of LPG vehicles were relatively low. However, the SOA/POA EFs of LPG vehicles ranged from 14 to 48, indicating that their POA EFs had a stronger effect, compared to the other fuel types.

Fig. 1 shows the real-time concentration changes of the aging aerosol and diluted exhaust gas in PAM during the experiment of the LPG vehicle LPI-ULEV #1 being driven in CVS-75. For the first 100 s after the initial start, the average THC-to-NO_x ($ppmC_{CVS}/ppm_{CVS}$) was 4.4, which subsequently increased to 76 by the end of Phase 1. In other words, the THC (avg. 9.1 $ppmC_{CVS}$), NO_x (avg. 2 ppm_{CVS}), and CO (avg. 113 ppm_{CVS}) were high until reaching the aftertreatment system entered stable operation, after the start reduced the OH exposure inside PAM. However, despite the high THC (avg. 9.1 $ppmC_{CVS}$), the high direct-NH_3 (avg. 20 ppm_{CVS}) and NO_x concentrations first produced ammonium nitrate, and the lower NO_x concentrations (avg. 0.1 ppm) and higher THC-to-NO_x ratio encouraged the formation of SOA. As a result, the Phase 1 (cold-started) SOA EFs of the LPG vehicles in CVS-75 increased from 1.9 to 1 mg kg-fuel^{-1} to 5.6 and 5.3 mg kg-fuel^{-1} in hot conditions (Phase 2). However, in NEDC, the SOA EFs were 12.2 and 7.2 mg kg-fuel^{-1} in Phase 1, including the initial start. They decreased to 8.9 and 3.4 mg kg-fuel^{-1} in Phase 2, under high-speed driving. Similarly, Karjalainen et al. (2016) reported that GDI gasoline vehicles driven in NEDC using PAM (1.03×10^{12} molecules cm^{-3} s of OH exposure) produced a SOA EF of 10.92 mg km^{-1}; this decreased to 0.52 mg km^{-1} in Phase 2. Although LPG and gasoline have different fuel characteristics, it is believed that the speed profile of NEDC did not differ significantly from CVS-75 during deceleration and rapid acceleration because their combustion and aftertreatment systems are similar. This would have allowed effective combustion control and purification, resulting in a low proportion of SOA precursors being emitted from incomplete combustion.

The SOA EFs of diesel vehicles varied by regulatory standard and by the combination of aftertreatment systems, among which EURO 6 (DOC + DPF + LNT (or SCR)) was the highest (24.5 mg kg-fuel^{-1} on average). This was followed by EURO 2–3 (non-DPF) at 19.8 mg kg-fuel^{-1} and

EURO 4–5 (DOC + DPF) at 14 mg kg-fuel^{-1}. SOA concentrations tended to vary with the regulatory mode, such that the regulatory mode of CVS-75 for EURO 2–3 diesel vehicles resulted in SOA EFs ranging from 2.4 to 49.8 mg kg-fuel^{-1}, whereas the non-regulatory mode of NEDC resulted in a higher SOA EF (approximately 4.5 mg kg-fuel^{-1}). The SOA EF/POA EF of EURO 2–3 was approximately 1.5, which was similar to the SOA/POA EF of 1.8 observed in the smog chamber study conducted by Gordon et al. (2014b) (3.5–7h of equivalent atmospheric aging), in which a medium-duty diesel vehicle (MDDV) was driven in CVS-75. Furthermore, the regulatory mode for EURO 4–6 diesel vehicles, NEDC, led to SOA EFs of 12.8–49.7 mg kg-fuel^{-1}; these values were up to 78 times higher than those of CVS-75 (0.4–31.5 mg kg-fuel^{-1}). DPF installation dramatically reduced the primary carbonaceous aerosols of diesel vehicles (POA and eBC). The improvement of the precursor purification rates in DOC and DPF, combined with the development of combustion technology, achieved a reduction in SOA compared to non-DPF diesel vehicles (Chirico et al., 2010; Gordon et al., 2013; Jathar et al., 2017; Karjalainen et al., 2019). As a result, in this study, diesel vehicles in EURO 4–5 equipped with DOC and DPF showed carbonaceous aerosol EFs (POA, eBC, SOA) that were 99.7% (for CVS-75) and 92% (for NEDC) lower than those of non-DPF vehicles. However, the proportion of SOA EFs rose to 0.4–36% for EURO 2–3 and 59–97% for EURO 4–5 vehicles. This phenomenon again increased for the proportion of SOA EFs to 97–99%. The addition of SCR (or LNT) aftertreatment systems reduced NO_x by 56%, compared to EURO 5. Also, the average SOA EF of EURO 6 increased to 19.8 mg kg-fuel^{-1} for CVS-75, and to 29.1 mg kg-fuel^{-1} for NEDC, or by 31 times and 1.2 times, respectively. This increase likely resulted from OH exposure of EURO 6, which ranged by phase during the experiment from 2.1 × 10^{10} to 9.9 × 10^{11} molecules cm^{-3} s; this was somewhat higher than that of EURO 5 when SOA was formed, and the yield of the precursors also increased due to the lower NO_x conditions in PAM. However, from the perspective of the corresponding NEDC regulatory mode, there was only a small significant change in SOA formation in EURO 6.

In this study, NO_x was found to be emitted from all of the fuel types with NO_x and NH_3, in a counter partner relationship. The nitrate EFs of gasoline vehicles (15.5–119 mg kg-fuel^{-1}) were higher than those of LPG vehicles (0.4–33 mg kg-fuel^{-1}); both fuel types emitted large amounts of NH_3 (Fig. 2c). This was consistent with the ranking trend reported by Link et al. (2017), though the results of diesel vehicles were different in this study. In Fig. 2c, direct-NH_3 emissions for diesel vehicles were below the equipment's limit of detection (LOD) of 0.2 ppm, except for the average 3.3 ppm of EURO 6-LNT #1 (Suarez-Bertoa et al., 2015). Nevertheless, the nitrate EFs (3.9–150) appeared to be caused by the influx of external NH_3 without being filtered at the pre-treatment system using diluted air during the experiment. In addition, the high NO_x conditions of the diesel vehicles (PAM input diluted NO_x: 0.3–26.3 ppm for diesel vehicles, 0.002–4.3 ppm for gasoline and LPG vehicles) may also have encouraged this formation.

3.3. Expected SOA yield and SOA/ΔCO

Fig. 4 shows the expected SOA yields calculated using profiles (Lee et al., 2015; Lu et al., 2018; Robinson et al., 2007; Zhao et al., 2015, 2016) of the SOA (μg m^{-3}), VOCs, and IVOCs measured during the different phases of each run. As VOCs and IVOCs emitted from the vehicles during the experiment may differ from the profiles used to calculate the expected SOA yields, any quantitative explanation of the changes under each regulatory standard is limited. However, the results of some of the regulated vehicles and cold and hot phases showed similar trends to those reported in previous studies.

The SOA with corrected POA and background concentrations ranged from 0.2 to 155 μg m^{-3} and was found to be lower with the cold-started (Phase 1) vehicles than the hot-started (Phases 2 and 3 for CVS-75 and NEDC) vehicles (Fig. S4). In addition, the expected SOA yield increased to approximately 0.93 overall as SOA increased, and this tendency was

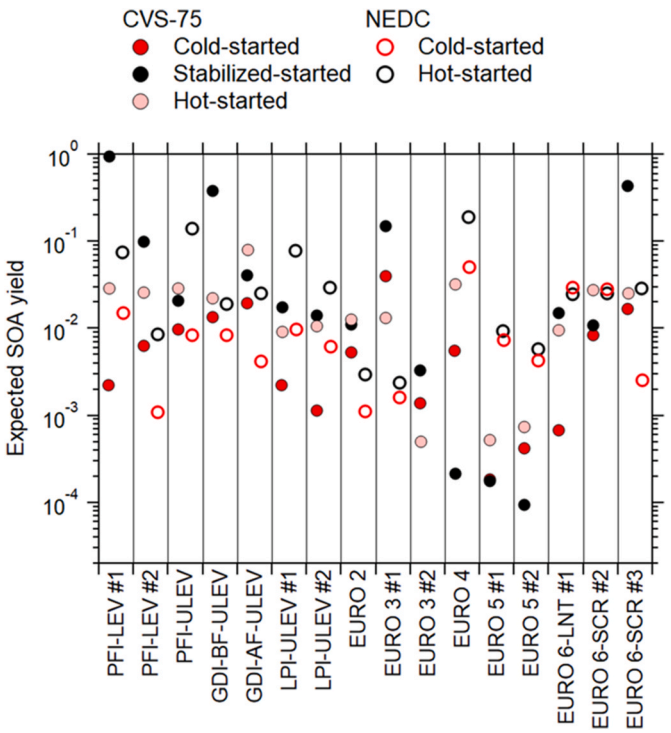

Fig. 4. Comparison of expected SOA yield for each phase according to Eq. (2). The SOA were corrected by background and POA values. Lu et al. (2018)'s profiles of VOCs and Zhao et al. (2016)'s profiles of IVOCs (LEV2) were applied for gasoline vehicles. VOC profiles are divided into cold-started and hot-started. LPG vehicles are shown with NIER's profile (Lee et al., 2015) of VOCs, including the cold-started and hot-started cases, as for gasoline vehicles. For diesel vehicles, VOCs are applied differently depending on the aftertreatment (DPF or non-DPF), referring to Lu et al. (2018). However, for IVOCs fraction, the profile of the non-DPF in Zhao et al. (2015)'s paper is applied here without this distinction. More detailed information of cold and hot-started vs. measured SOA is provided in Fig. S5.

consistent with the trends in other smog chambers and PAM studies on vehicles (Jathar et al., 2017; Pieber et al., 2018; Platt et al., 2017; Zhao et al., 2018). In particular, the cold-start results for the gasoline vehicles in this study were low regardless of the driving mode, which was in line with the findings of Zhao et al. (2018). It should be noted that, as the domestic NMOG standard for gasoline vehicles was tightened and the PM regulation for GDI vehicles began, the cold-start NMOG of the corresponding regulation mode (CVS-75) increased from 0.002 to 0.019, and the SOA (EF) also increased from 23 μg m^{-3} (12 mg kg-fuel^{-1}) to 98 μg m^{-3} (58 mg kg-fuel^{-1}), except for PFI-LEV #2. This is because of the enhanced combustion control technology, which prevents excessive exhaust emissions during the initial start and the achievement of fast, optimal purification rates of aftertreatment systems, which reduces POAs. While the NMOG (or NMHC) EF during the cold start in this study decreased from 184 mg km^{-1} to 59 mg km^{-1}, the actual composition of the SOA precursors was not significantly affected by the reduced NMOG (or NMHC) (May et al., 2014; Saliba et al., 2017; Zhao et al., 2017). This trend, despite being cold-started, is consistent with the overall changes in SOA yields for gasoline vehicles for each regulatory standard, as reported by Zhao et al. (2017). In addition, the expected SOA yield during the hot-start was higher than that during the cold start, which can be attributed to the relatively higher OH exposure conditions and the increased IVOCs in NMOG (or NMHC) (Zhao et al., 2016, 2018).

The LPG vehicles were lower during the cold start, similar to the gasoline vehicles, and the tendency for the expected SOA yield to increase with increasing SOA concentrations was identical to that of the other fuel types (Fig. S4). Under similar OH exposure conditions by fuel type, the NEDC hot-start results of the LPG vehicles reached the same

level as those of the gasoline and DPF-equipped diesel vehicles (EURO 4–6). Therefore, while LPG vehicles produce less SOA during high-speed driving without rapid speed changes, such as acceleration and deceleration, they may still contribute significantly to SOA regarding their overall composition. However, further research is necessary into the SOA precursors mentioned above, to obtain a more accurate comparison.

Depending on the emission regulation standard, DPF installation, and additional NO_x-reducing aftertreatment device, the expected SOA yield increased from ~0.15 (~7.6×10^{11} molecules cm^{-3} s) in EURO 2–3 (non-DPF), to 0.19 (~6.4×10^{11} molecules cm^{-3} s) in EURO 4–5 (DPF), and then to ~0.43 (~7.2×10^{11} molecules cm^{-3} s) in EURO 6 (DPF, LNT, or SCR). At the same time, the NMHC-to-NO_x ratios (ppmC/ppm) from PAM ranged from 0.03 to 0.19, 0.03–1.56, and 0.09–2.8, respectively, indicating an increasing fraction of NMHC. In addition, with the tightening of regulations, NO_x and NMHC EFs decreased from ~1600 mg km^{-1} to ~400 mg km^{-1} and from ~76 mg km^{-1} to ~30 mg km^{-1}, respectively, during the PAM experiment. While a direct NMHC composition analysis could not be conducted, the consistent trend in the expected SOA yields of the diesel vehicles was an interesting result. However, this study does not represent all diesel vehicles, as it only examined passenger vehicles. Therefore, other diesel vehicles that contribute to emissions significantly, such as diesel cargo vehicles, should also be investigated.

Fig. 5 shows SOA/ΔCO with respect to changing equivalent photochemical age [OH] (hereafter eq. age) for each fuel type. SOA/ΔCO is used to evaluate the effect of SOA from combustion emissions across an area or at the source (traffic and biomass) by using ΔCO (background corrected) as a tracer to normalize the dilution effect (DeCarlo et al., 2010; de Gouw et al., 2008). Within the OH_{exp} range simulated in this study, the gasoline, LPG, and EURO 4–6 (with DPF) diesel vehicles showed increasing SOA/ΔCO ratios with increasing eq. age (more information in Fig. S6). In addition, for a similar eq. age (~6), the SOA/ΔCO for gasoline vehicles was 30 $\mu g\ m^{-3}\ ppm^{-1}$ (~5 eq. age), which was higher than those of LPG vehicles at 6 $\mu g\ m^{-3}\ ppm^{-1}$ (~6 eq. age) and EURO 4–6 (with DPF) diesel vehicles at 12 $\mu g\ m^{-3}\ ppm^{-1}$ (~4 eq. age). However, except for EURO 2–3 (without DPF) diesel vehicles at 0.7–1.1 $\mu g\ m^{-3}\ ppm^{-1}$ at 1 eq. age, their ratios were distributed across a range of 0.7–1.1 $\mu g\ m^{-3}\ ppm^{-1}$ at 4–6 eq. age. As shown in Fig. 5, the corrected CO ranged from 0.1 to 281 ppm for gasoline vehicles, 1.1–24.4 ppm for LPG vehicles, 0.1–9.6 ppm for EURO 4–6 (without DPF) diesel vehicles, and 0.1–16.4 ppm for EURO 2–3 (without DPF). This indicates that gasoline and LPG vehicles had higher CO emissions, possibly due to their aftertreatment system characteristics. Therefore, the emission effects of the dominant fuel types should be considered when comparing the SOA/ΔCO effect in the atmosphere, particularly in areas with concentrated vehicle sources. Furthermore, as various vehicle models were grouped in this study to examine the SOA/ΔCO tendency by the eq. age of each fuel type, multiple factors in the formation of SOA were combined together, such as combustion technology, displacement, aftertreatment system, regulatory standard, and driving mode. Therefore, these implicit factors should be considered when applying the results of this study.

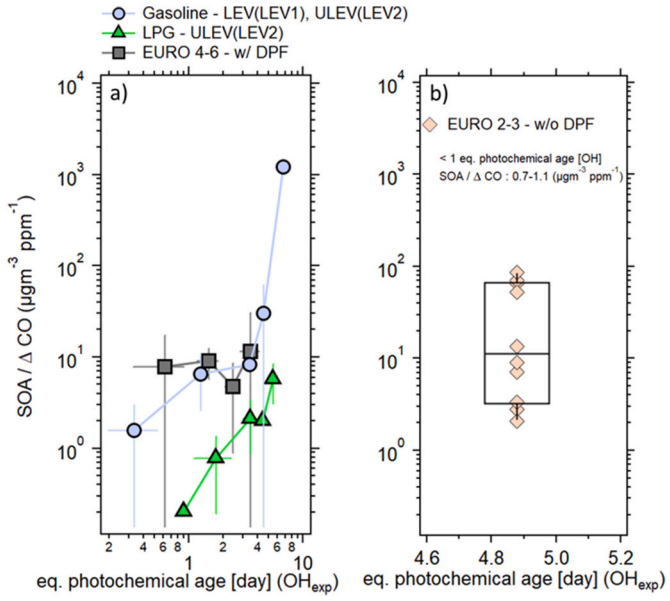

Fig. 5. Ratio of SOA/ΔCO vs. eq. photochemical age [day] (OHexp = 1.5×10^6 molec. cm^{-3} in an atmospheric day). a) Gasoline (LEVs-LEV1, ULEVs-LEV2), LPG (ULEVs-LEV2), and EURO 4–6 (w/DPF); number of phases as follows: n = 25 for gasoline, n = 10 for LPG, and n = 18 for diesel vehicles. b) Box plot of EURO 2–3 (w/o DPF, n = 10 phases); the top, middle, and bottom lines of the boxes show the 75th, 50th, and 25th percentiles, respectively and whiskers show the 10th and 90th percentiles. More detailed information of raw SOA/ΔCO is presented in Fig. S6.

4. Conclusion

Here, the primary gases, primary aerosols, and secondary aerosols produced in PAM were analyzed according to the regulatory standards of domestic passenger vehicles, using the most common fuel types in South Korea (gasoline, LPG, and diesel). In this study, the fate of the LVOCs method suggested by Palm et al. (2016) could not be applied to reflect the effect of the partitioning process of LVOCs during SOA formation. As in other previous studies, as direct-NH_3 was found to be high for gasoline and LPG vehicles (maximum average of ~34 ppm), which are not currently regulated for NH_3 in South Korea (only regulation is below 10 ppm NH_3 average for large and extra-large passengers and cargo vehicles), additional research is required for these unregulated vehicles considering the nitrate results shown in Fig. 3 (Jordan et al., 2020; Link et al., 2017; Park et al., 2019; Suarez-Bertoa et al., 2015).

Considering the existing lack of research on SOA from LPG vehicles, the lower SOA EFs (3–11 mg kg-$fuel^{-1}$) of LPG vehicles, compared to gasoline and diesel vehicles (EURO 4–6), obtained using PAM in this study is expected to increase the relative usefulness of environment assessments, particularly at a time when the purchase eligibility of LPG vehicles has been eased. However, direct-NH_3 was found to potentially cause the formation of ammonium nitrate (Figs. 1 and 2), and eBC, which causes global warming. The average expected SOA yield of 0.05 (~16.4 μg m^{-3} of SOA measured) was similar to those of gasoline and diesel vehicles (EURO 4–6) during the formation of SOA under hot conditions (Figs. 3 and 4). Furthermore, the SOA/ΔCO levels increased with increasing eq. age (Fig. 5); this requires further research focusing on the emissions and SOA, using more diverse vehicle models and different driving conditions for LPG vehicles.

The expected SOA yield was found to be lower during cold-start than hot-start conditions; this finding was consistent with previous studies (see caption for Fig. 4) (Zhao et al., 2016, 2018). Installing DPFs into diesel vehicles drastically reduces primary carbonaceous aerosols and SOA, as demonstrated in this study. Here, EURO 4–6 diesel vehicles were found to be up to 95% lower than non-DPF EURO 2–3 vehicles In this regard. However, the expected SOA yield appeared to increase with tightening regulation. Based on this study, the NMHC-to-NO_x ratio and NO_x concentration condition affected the changing precursor yield. Furthermore, the relatively smaller reduction in oxygenates (C_9 to C_{27}) from fuel and lubricant oil emissions was attributed to the combination of the decreased NMHC (from ~76 mg km^{-1} to ~30 mg km^{-1} in this measurement) and the enhanced aftertreatment system. This led to higher oxidation of the catalysts (Karjalainen et al., 2019; Liu et al., 2020; Zeraati-Rezaei et al., 2020). However, as the profiles from previous studies were adopted in this study, the actual results may have been different, and there are currently insufficient data on large cargo diesel vehicles with a high displacement; further research is required in

this regard.

As the SOA/ΔCO, shown in Fig. 5, was obtained based on limited driving conditions and a simplified comparison between the fuel types, the results of this study may differ from reality due to the complex combination of the actual factors. However, considering the lack of comparative evaluation of secondary air pollution from domestic vehicles, this study provides valuable regulatory data, which could be used to evaluate the atmospheric effects of each fuel type, albeit partially, using the relative differences in the formation of SOA from the combustion of individual fuel types.

The driving conditions and fuel properties can vary depending on the seasonal temperature (e.g., summer or winter) as well as the lubricant oil used. These factors will affect the composition and fractions of the dominant chemicals during the formation of SOA (Gordon et al., 2014b; Liu et al., 2020; Platt et al., 2017). Therefore, these seasonal aspects should be further investigated in the future. Comparative evaluations using modern emission evaluation methods, such as real driving emission (RDE) and the worldwide harmonized light vehicle test procedure (WLTP), should continue to be conducted with a view to the evolution of low-emission passenger vehicles.

Credit statement

Gyutae Park: conceptualization, methodology, data analysis, investigation, writing-original draft **Kyunghoon Kim**: methodology, data analysis, investigation **Taehyun Park:** methodology, formal analysis **Seokwon Kang:** formal analysis, installation vehicles on chassis dynamometer **Jihee Ban:** formal analysis, installation vehicles on chassis dynamometer **Siyoung Choi:** formal analysis **Dong-Gil Yu:** investigation **Sanguk Lee:** resources **Yunsung Lim:** resources, **Sunmoon Kim:** resources **Sunhee Mun:** data analysis **Jung-Hun Woo:** formal analysis **Chan-Soo Jeon:** formal analysis **Taehyoung Lee:** conceptualization, project administration, supervision, writing-original draft.

Declaration of competing interest

The authors declare that they have no known competing financial interests or personal relationships that could have appeared to influence the work reported in this paper.

Acknowledgments

We thank the research scientists at the Transportation Pollution Research Center. This work was supported by a grant from the National Institute of Environment Research (NIER), funded by the Ministry of Environment (MOE) of the Republic of Korea (NIER-2019-04-02-018). This research has not been officially reviewed by the MOE. Additional data analysis was supported by the Korea Environment Industry & Technology Institute (KEITI) through the Public Technology Program based on the Environmental Policy Program, funded by the Korea Ministry of Environment (MOE) (2019000160007). The extended experiment was conducted by the Korea Basic Science Institute (National Research Facilities and Equipment Center) grant, funded by the Ministry of Education (2019R1A6C1020041). The views expressed in the research are solely the authors' views, and do not necessarily reflect the MOE's view. This research was conducted on small vehicles, and does not represent the results for all vehicles in South Korea.

Appendix A. Supplementary data

Supplementary data to this article can be found online at https://doi.org/10.1016/j.envpol.2021.117195.

References

Chirico, R., DeCarlo, P.F., Heringa, M.F., Tritscher, T., Richter, R., Prévôt, A.S.H., Dommen, J., Weingartner, E., Wehrle, G., Gysel, M., Laborde, M., Baltensperger, U., 2010. Impact of aftertreatment devices on primary emissions and secondary organic aerosol formation potential from in-use diesel vehicles: results from smog chamber experiments. Atmos. Chem. Phys. 10, 11545–11563. https://doi.org/10.5194/acp-10-11545-2010.

Choi, Y., Lee, J., Jang, J., Park, S., 2019. Effects of fuel-injection systems on particle emission characteristics of gasoline vehicles Atmos. Environ. Times 217, 116941. https://doi.org/10.1016/j.atmosenv.2019.116941.

de Gouw, J.A., Brock, C.A., Atlas, E.L., Bates, T.S., Fehsenfeld, F.C., Goldan, P.D., Holloway, J.S., Kuster, W.C., Lerner, B.M., Matthew, B.M., Middlebrook, A.M., Onasch, T.B., Peltier, R.E., Quinn, P.K., Senff, C.J., Stohl, A., Sullivan, A.P., Trainer, M., Warneke, C., Weber, R.J., Williams, E.J., 2008. Sources of particulate matter in the northeastern United States in summer: 1. Direct emissions and secondary formation of organic matter in urban plumes. J. Geophys. Res. Atmos. 113 https://doi.org/10.1029/2007jd009243.

DeCarlo, P.F., Kimmel, J.R., Trimborn, A., Northway, M.J., Jayne, J.T., Aiken, A.C., Gonin, M., Fuhrer, K., Horvath, T., Docherty, K.S., Worsnop, D.R., Jimenez, J.L., 2006. Field-deployable, high-resolution, time-of-flight aerosol mass spectrometer. Anal. Chem. 78, 8281–8289. https://doi.org/10.1021/ac061249n.

DeCarlo, P.F., Ulbrich, I.M., Crounse, J., de Foy, B., Dunlea, E.J., Aiken, A.C., Knapp, D., Weinheimer, A.J., Campos, T., Wennberg, P.O., Jimenez, J.L., 2010. Investigation of the sources and processing of organic aerosol over the Central Mexican Plateau from aircraft measurements during MILAGRO. Atmos. Chem. Phys. 10, 5257–5280. https://doi.org/10.5194/acp-10-5257-2010.

Deng, W., Fang, Z., Wang, Z., Zhu, M., Zhang, Y., Tang, M., Song, W., Lowther, S., Huang, Z., Jones, K., Peng, P.a., Want, X., 2020. Primary emissions and secondary organic aerosol formation from in-use diesel vehicle exhaust: comparison between idling and cruise mode. Sci. Total Environ. 699, 134357. https://doi.org/10.1016/j.scitotenv.2019.134357.

Du, Z., Hu, M., Peng, J., Zhang, W., Zheng, J., Gu, F., Qin, Y., Yang, Y., Li, M., Wu, Y., Shao, M., Shuai, S., 2018. Comparison of primary aerosol emission and secondary aerosol formation from gasoline direct injection and port fuel injection vehicles. Atmos. Chem. Phys. 18, 9011–9023. https://doi.org/10.5194/acp-18-9011-2018.

George, I.J., Hays, M.D., Herrington, J.S., Preston, W., Snow, R., Faircloth, J., George, B. J., Long, T., Baldauf, R.W., 2015. Effects of cold temperature and ethanol content on VOC emissions from light-duty gasoline vehicles. Environ. Sci. Technol. 49, 13067–13074. https://doi.org/10.1021/acs.est.5b04102.

Giani, P., Balzarini, A., Pirovano, G., Gilardoni, S., Paglione, M., Colombi, C., Gianelle, V. L., Belis, C.A., Poluzzi, V., Lonati, G., 2019. Influence of semi-and intermediate-volatile organic compounds (S/IVOC) parameterizations, volatility distributions and aging schemes on organic aerosol modelling in winter conditions. Atmos. Environ. 213, 11–24. https://doi.org/10.1016/j.atmosenv.2019.05.061.

Gordon, T., Presto, A., May, A., Nguyen, N., Lipsky, E., Donahue, N., Gutierrez, A., Zhang, M., Maddox, C., Rieger, P., 2014a. Secondary organic aerosol formation exceeds primary particulate matter emissions for light-duty gasoline vehicles. Atmos. Chem. Phys. 14, 4661–4678. https://doi.org/10.5194/acp-14-4661-2014.

Gordon, T.D., Presto, A.A., Nguyen, N.T., Robertson, W.H., Na, K., Sahay, K.N., Zhang, M., Maddox, C., Rieger, P., Chattopadhyay, S., Maldonado, H., Maricq, M.M., Robinson, A.L., 2014b. Secondary organic aerosol production from diesel vehicle exhaust: impact of aftertreatment, fuel chemistry and driving cycle. Atmos. Chem. Phys. 14, 4643–4659. https://doi.org/10.5194/acp-14-4643-2014.

Gordon, T.D., Tkacik, D.S., Presto, A.A., Zhang, M., Jathar, S.H., Nguyen, N.T., Massetti, J., Truong, T., Cicero-Fernandez, P., Maddox, C., Rieger, P., Chattopadhyay, S., Maldonado, H., Maricq, M.M., Robinson, A.L., 2013. Primary gas- and particle-phase emissions and secondary organic aerosol production from gasoline and diesel off-road engines. Environ. Sci. Technol. 47, 14137–14146. https://doi.org/10.1021/es403556e.

Heal, M.R., Kumar, P., Harrison, R.M., 2012. Particles, air quality, policy and health. Chem. Soc. Rev. 41, 6606–6630. https://doi.org/10.1039/C2CS35076A.

Hu, W., Palm, B.B., Day, D.A., Campuzano-Jost, P., Krechmer, J.E., Peng, Z., de Sá, S.S., Martin, S.T., Alexander, M.L., Baumann, K., Hacker, L., Kiendler-Scharr, A., Koss, A. R., de Gouw, J.A., Goldstein, A.H., Seco, R., Sjostedt, S.J., Park, J.H., Guenther, A.B., Kim, S., Canonaco, F., Prévôt, A.S.H., Brune, W.H., Jimenez, J.L., 2016. Volatility and lifetime against OH heterogeneous reaction of ambient isoprene-epoxydiols-derived secondary organic aerosol (IEPOX-SOA). Atmos. Chem. Phys. 16, 11563–11580. https://doi.org/10.5194/acp-16-11563-2016.

Jathar, S.H., Friedman, B., Galang, A.A., Link, M.F., Brophy, P., Volckens, J., Eluri, S., Farmer, D.K., 2017. Linking load, fuel, and emission controls to photochemical production of secondary organic aerosol from a diesel engine. Environ. Sci. Technol. 51, 1377–1386. https://doi.org/10.1021/acs.est.6b04602.

Jathar, S.H., Gordon, T.D., Hennigan, C.J., Pye, H.O., Pouliot, G., Adams, P.J., Donahue, N.M., Robinson, A.L., 2014. Unspeciated organic emissions from combustion sources and their influence on the secondary organic aerosol budget in the United States. Proc. Natl. Acad. Sci. U.S.A. 111, 10473–10478. https://doi.org/10.1073/pnas.1323740111.

Jordan, C.E., Crawford, J.H., Beyersdorf, A.J., Eck, T.F., Halliday, H.S., Nault, B.A., Chang, L.-S., Park, J., Park, R., Lee, G., Kim, H., Ahn, J., Cho, S., Shin, H.J., Lee, J.H., Jung, J., Kim, D.-S., Lee, M., Lee, T., Whitehill, A., Szykman, J., Schueneman, M.K., Campuzano-Jost, P., Jimenez, J.L., DiGangi, J.P., Diskin, G.S., Anderson, B.E., Moore, R.H., Ziemba, L.D., Fenn, M.A., Hair, J.W., Kuehn, R.E., Holz, R.E., Chen, G., Travis, K., Shook, M., Peterson, D.A., Lamb, K.D., Schwarz, J.P., 2020. Investigation of factors controlling PM 2.5 variability across the South Korean Peninsula during KORUS-AQ. Elem Sci Anth 8 (1), 28. https://doi.org/10.1525/elementa.424, 2020.

Kang, E., Root, M.J., Toohey, D.W., Brune, W.H., 2007. Introducing the concept of potential aerosol mass (PAM). Atmos. Chem. Phys. 7, 5727–5744. https://doi.org/10.5194/acp-7-5727-2007.

Kang, E., Toohey, D.W., Brune, W.H., 2011. Dependence of SOA oxidation on organic aerosol mass concentration and OH exposure: experimental PAM chamber studies. Atmos. Chem. Phys. 11, 1837–1852. https://doi.org/10.5194/acp-11-1837-2011.

Karjalainen, P., Rönkkö, T., Simonen, P., Ntziachristos, L., Juuti, P., Timonen, H., Teinilä, K., Saarikoski, S., Saveljeff, H., Lauren, M., Happonen, M., Matilainen, P., Maunula, T., Nuottimäki, J., Keskinen, J., 2019. Strategies to diminish the emissions of particles and secondary aerosol formation from diesel engines. Environ. Sci. Technol. 53, 10408–10416. https://doi.org/10.1021/acs.est.9b04073.

Karjalainen, P., Timonen, H., Saukko, E., Kuuluvainen, H., Saarikoski, S., Aakko-Saksa, P., Murtonen, T., Bloss, M., Dal Maso, M., Simonen, P., Ahlberg, E., Svenningsson, B., Brune, W.H., Hillamo, R., Keskinen, J., Rönkkö, T., 2016. Time-resolved characterization of primary particle emissions and secondary particle formation from a modern gasoline passenger car. Atmos. Chem. Phys. 16, 8559–8570. https://doi.org/10.5194/acp-16-8559-2016.

Korea Energy Agency, 2014. Study on Establishment of Standard of '14 Calorific Value and Carbon Emission Factor of Domestic Energy Sources. Available from. http://www.kemco.or.kr/web/kem_home_new/introduce/public/etc/resch/kem_view.asp?q=19203.

Lambe, A.T., Ahern, A.T., Williams, L.R., Slowik, J.G., Wong, J.P.S., Abbatt, J.P.D., Brune, W.H., Ng, N.L., Wright, J.P., Croasdale, D.R., Worsnop, D.R., Davidovits, P., Onasch, T.B., 2011. Characterization of aerosol photooxidation flow reactors: heterogeneous oxidation, secondary organic aerosol formation and cloud condensation nuclei activity measurements. Atmos. Meas. Tech. 4, 445–461. https://doi.org/10.5194/amt-4-445-2011.

Lee, J., Kim, S., Son, J., Yoo, H.M., Yoon, C., Koh, J., Mun, S., Park, G., Chung, T., Lee, S., Lee, T., Park, S., Yoon, S., Lee, S., Shin, Y., 2015. Annual Research on the Emission Characteristics of Mobile Source Air Toxics and Management Strategy (II). Transportation pollution research center.

Li, R., Palm, B.B., Ortega, A.M., Hlywiak, J., Hu, W., Peng, Z., Day, D.A., Knote, C., Brune, W.H., de Gouw, J.A., Jimenez, J.L., 2015. Modeling the radical chemistry in an oxidation flow reactor: radical formation and recycling, sensitivities, and the OH exposure estimation equation. J. Phys. Chem. 119, 4418–4432. https://doi.org/10.1021/jp509534k.

Link, M.F., Kim, J., Park, G., Lee, T., Park, T., Babar, Z.B., Sung, K., Kim, P., Kang, S., Kim, J.S., Choi, Y., Son, J., Lim, H.-J., Farmer, D.K., 2017. Elevated production of NH_4NO_3 from the photochemical processing of vehicle exhaust: implications for air quality in the Seoul Metropolitan Region. Atmos. Environ. 156, 95–101. https://doi.org/10.1016/j.atmosenv.2017.02.031.

Liu, H., Qi, L., Liang, C., Deng, F., Man, H., He, K., 2020. How aging process changes characteristics of vehicle emissions? A review. Crit. Rev. Environ. Sci. Technol. 50, 1796–1828. https://doi.org/10.1080/10643389.2019.1669402.

Liu, T., Zhou, L., Liu, Q., Lee, B.P., Yao, D., Lu, H., Lyu, X., Guo, H., Chan, C.K., 2019. Secondary organic aerosol formation from urban roadside air in Hong Kong. Environ. Sci. Technol. 53, 3001–3009. https://doi.org/10.1021/acs.est.8b06587.s001.

Lu, Q., Zhao, Y., Robinson, A.L., 2018. Comprehensive organic emission profiles for gasoline, diesel, and gas-turbine engines including intermediate and semi-volatile organic compound emissions. Atmos. Chem. Phys. 18, 17637–17654. https://doi.org/10.5194/acp-18-17637-2018.

Mao, J., Ren, X., Brune, W.H., Olson, J.R., Crawford, J.H., Fried, A., Huey, L.G., Cohen, R.C., Heikes, B., Singh, H.B., Blake, D.R., Sachse, G.W., Diskin, G.S., Hall, S.R., Shetter, R.E., 2009. Airborne measurement of OH reactivity during INTEX-B. Atmos. Chem. Phys. 9, 163–173. https://doi.org/10.5194/acp-9-163-2009.

May, A.A., Nguyen, N.T., Presto, A.A., Gordon, T.D., Lipsky, E.M., Karve, M., Gutierrez, A., Robertson, W.H., Zhang, M., Brandow, C., Chang, O., Chen, S., Cicero-Fernandez, P., Dinkins, L., Fuentes, M., Huang, S.-M., Ling, R., Long, J., Maddox, C., Massetti, J., McCauley, E., Miguel, A., Na, K., Ong, R., Pang, Y., Rieger, P., Sax, T., Truong, T., Vo, T., Chattopadhyay, S., Maldonado, H., Maricq, M.M., Robinson, A.L., 2014. Gas- and particle-phase primary emissions from in-use, on-road gasoline and diesel vehicles. Atmos. Environ. 88, 247–260. https://doi.org/10.1016/j.atmosenv.2014.01.046.

MOE, 2019. Special Act on the Reduction and Management of Fine Dust. .. Available from URL: https://www.law.go.kr/LSW/eng/engLsSc.do?menuId=2&section=lawNm&query=Special+Act+on+the+Reduction+and+Management+of+Fine+Dust&x=0&y=0#liBgcolor1

Myung, C.-L., Kim, J., Choi, K., Hwang, I.G., Park, S., 2012. Comparative study of engine control strategies for particulate emissions from direct injection light-duty vehicle fueled with gasoline and liquid phase liquefied petroleum gas (LPG). Fuel 94, 348–355. https://doi.org/10.1016/j.fuel.2011.10.041.

Myung, C.-L., Ko, A., Lim, Y., Kim, S., Lee, J., Choi, K., Park, S., 2014. Mobile source air toxic emissions from direct injection spark ignition gasoline and LPG passenger car under various in-use vehicle driving modes in Korea. Fuel Process. Technol. 119, 19–31. https://doi.org/10.1016/j.fuproc.2013.10.013.

Nault, B.A., Campuzano-Jost, P., Day, D.A., Schroder, J.C., Anderson, B., Beyersdorf, A.J., Blake, D.R., Brune, W.H., Choi, Y., Corr, C.A., de Gouw, J.A., Dibb, J., DiGangi, J.P., Diskin, G.S., Fried, A., Huey, L.G., Kim, M.J., Knote, C.J., Lamb, K.D., Lee, T., Park, T., Pusede, S.E., Scheuer, E., Thornhill, K.L., Woo, J.H., Jimenez, J.L., 2018. Secondary organic aerosol production from local emissions dominates the organic aerosol budget over Seoul, South Korea, during KORUS-AQ. Atmos. Chem. Phys. 18, 17769–17800. https://doi.org/10.5194/acp-18-17769-2018.

Odum, J.R., Hoffmann, T., Bowman, F., Collins, D., Flagan, R.C., Seinfeld, J.H., 1996. Gas/particle partitioning and secondary organic aerosol yields. Environ. Sci. Technol. 30, 2580–2585. https://doi.org/10.1021/es950943+.

Palm, B.B., Campuzano-Jost, P., Ortega, A.M., Day, D.A., Kaser, L., Jud, W., Karl, T., Hansel, A., Hunter, J.F., Cross, E.S., Kroll, J.H., Peng, Z., Brune, W.H., Jimenez, J.L., 2016. In situ secondary organic aerosol formation from ambient pine forest air using an oxidation flow reactor. Atmos. Chem. Phys. 16, 2943–2970. https://doi.org/10.5194/acp-16-2943-2016.

Park, G., Kim, K., Park, T., Kang, S., Ban, J., Choi, S., Yu, D.-G., Lee, S., Lim, Y., Kim, S., Lee, J., Woo, J.-H., Lee, T., 2020. Characterizing black carbon emissions from gasoline, LPG, and diesel vehicles via transient chassis-dynamometer tests. Appl. Sci. 10, 5856. https://doi.org/10.3390/app10175856.

Park, G., Mun, S., Hong, H., Chung, T., Jung, S., Kim, S., Seo, S., Kim, J., Lee, J., Kim, K., Park, T., Kang, S., Ban, J., Yu, D.-G., Woo, J.-H., Lee, T., 2019. Characterization of emission factors concerning gasoline, LPG, and diesel vehicles via transient chassis-dynamometer tests. Appl. Sci. 9, 1573. https://doi.org/10.3390/app9081573.

Pieber, S.M., Kumar, N.K., Klein, F., Comte, P., Bhattu, D., Dommen, J., Bruns, E.A., Kılıç, D., El Haddad, I., Keller, A., Czerwinski, J., Heeb, N., Baltensperger, U., Slowik, J.G., Prévôt, A.S.H., 2018. Gas-phase composition and secondary organic aerosol formation from standard and particle filter-retrofitted gasoline direct injection vehicles investigated in a batch and flow reactor. Atmos. Chem. Phys. 18, 9929–9954. https://doi.org/10.5194/acp-18-9929-2018.

Platt, S.M., El Haddad, I., Pieber, S.M., Zardini, A.A., Suarez-Bertoa, R., Clairotte, M., Daellenbach, K.R., Huang, R.J., Slowik, J.G., Hellebust, S., Temime-Roussel, B., Marchand, N., de Gouw, J., Jimenez, J.L., Hayes, P.L., Robinson, A.L., Baltensperger, U., Astorga, C., Prévôt, A.S.H., 2017. Gasoline cars produce more carbonaceous particulate matter than modern filter-equipped diesel cars. Sci. Rep. 7, 4926. https://doi.org/10.1038/s41598-017-03714-9.

Robinson, A.L., Donahue, N.M., Shrivastava, M.K., Weitkamp, E.A., Sage, A.M., Grieshop, A.P., Lane, T.E., Pierce, J.R., Pandis, S.N., 2007. Rethinking organic aerosols: semivolatile emissions and photochemical aging. Science 315, 1259–1262. https://doi.org/10.1126/science.1133061.

Saha, P.K., Khlystov, A., Snyder, M.G., Grieshop, A.P., 2018a. Characterization of air pollutant concentrations, fleet emission factors, and dispersion near a North Carolina interstate freeway across two seasons. Atmos. Environ. 177, 143–153. https://doi.org/10.1016/j.atmosenv.2018.01.019.

Saha, P.K., Reece, S.M., Grieshop, A.P., 2018b. Seasonally varying secondary organic aerosol formation from in-situ oxidation of near-highway air. Environ. Sci. Technol. 52, 7192–7202. https://doi.org/10.1021/acs.est.8b01134.

Saliba, G., Saleh, R., Zhao, Y., Presto, A.A., Lambe, A.T., Frodin, B., Sardar, S., Maldonado, H., Maddox, C., May, A.A., Drozd, G.T., Goldstein, A.H., Russell, L.M., Hagen, F., Robinson, A.L., 2017. Comparison of gasoline direct-injection (GDI) and port fuel injection (PFI) vehicle emissions: emission certification standards, cold-start, secondary organic aerosol formation potential, and potential climate impacts. Environ. Sci. Technol. 51, 6542–6552. https://doi.org/10.1021/acs.est.6b06509.

Shah, R.U., Coggon, M.M., Gkatzelis, G., McDonald, B., Tasoglou, A., Huber, H., Gilman, J.B., Warneke, C., Robinson, A.L., Presto, A.A., 2019. Urban oxidation flow reactor measurements reveal significant secondary organic aerosol contributions from volatile emissions of emerging importance. Environ. Sci. Technol. 54, 714–725. https://doi.org/10.1021/acs.est.9b06531.

Suarez-Bertoa, R., Zardini, A.A., Lilova, V., Meyer, D., Nakatani, S., Hibel, F., Ewers, J., Clairotte, M., Hill, L., Astorga, C., 2015. Intercomparison of real-time tailpipe ammonia measurements from vehicles tested over the new world-harmonized light-duty vehicle test cycle (WLTC). Environ. Sci. Pollut. Res. 22, 7450–7460. https://doi.org/10.1007/s11356-015-4267-3.

Tkacik, D.S., Lambe, A.T., Jathar, S., Li, X., Presto, A.A., Zhao, Y., Blake, D., Meinardi, S., Jayne, J.T., Croteau, P.L., Robinson, A.L., 2014. Secondary organic aerosol formation from in-use motor vehicle emissions using a potential aerosol mass reactor. Environ. Sci. Technol. 48, 11235–11242. https://doi.org/10.1021/es502239v.

Yeom, K., Jang, J., Bae, C., 2007. Homogeneous charge compression ignition of LPG and gasoline using variable valve timing in an engine. Fuel 86, 494–503. https://doi.org/10.1016/j.fuel.2006.07.027.

Ylisirniö, A., Buchholz, A., Mohr, C., Li, Z., Barreira, L., Lambe, A., Faiola, C., Kari, E., Yli-Juuti, T., Nizkorodov, S.A., Worsnop, D.R., Virtanen, A., Schobesberger, S., 2020. Composition and volatility of secondary organic aerosol (SOA) formed from oxidation of real tree emissions compared to simplified volatile organic compound (VOC) systems. Atmos. Chem. Phys. 20, 5629–5644. https://doi.org/10.5194/acp-20-5629-2020.

Zeraati-Rezaei, S., Alam, M.S., Xu, H., Beddows, D.C., Harrison, R.M., 2020. Size-resolved physico-chemical characterization of diesel exhaust particles and efficiency of exhaust aftertreatment. Atmos. Environ. 222, 117021. https://doi.org/10.1016/j.atmosenv.2019.117021.

Zhao, Y., Lambe, A.T., Saleh, R., Saliba, G., Robinson, A.L., 2018. Secondary organic aerosol production from gasoline vehicle exhaust: effects of engine technology, cold start, and emission certification standard. Environ. Sci. Technol. 52, 1253–1261. https://doi.org/10.1021/acs.est.7b05045.

Zhao, Y., Nguyen, N.T., Presto, A.A., Hennigan, C.J., May, A.A., Robinson, A.L., 2015. Intermediate volatility organic compound emissions from on-road diesel vehicles: chemical composition, emission factors, and estimated secondary organic aerosol production. Environ. Sci. Technol. 49, 11516–11526. https://doi.org/10.1021/acs.est.5b02841.

Zhao, Y., Nguyen, N.T., Presto, A.A., Hennigan, C.J., May, A.A., Robinson, A.L., 2016. Intermediate volatility organic compound emissions from on-road gasoline vehicles and small off-road gasoline engines. Environ. Sci. Technol. 50, 4554–4563. https://doi.org/10.1021/acs.est.5b06247.

Zhao, Y., Saleh, R., Saliba, G., Presto, A.A., Gordon, T.D., Drozd, G.T., Goldstein, A.H., Donahue, N.M., Robinson, A.L., 2017. Reducing secondary organic aerosol

formation from gasoline vehicle exhaust. Proc. Natl. Acad. Sci. U.S.A. 114, 6984–6989. https://doi.org/10.1073/pnas.1620911114.